Discoidal Impressions and Trace-Like Fossils More Than 1200 Million Years Old

Birger Rasmussen,[1]* Stefan Bengtson,[2] Ian R. Fletcher,[1] Neal J. McNaughton[1]

The Stirling Range Formation of southwestern Australia contains discoidal impressions and trace-like fossils in tidal sandstones. The various disks have previously been linked to the Ediacaran biota, younger than 600 million years old. From this unit, we report U-Th-Pb geochronology of detrital zircon and monazite, as well as low-grade metamorphic monazite, constraining the depositional age to between 2016 ± 6 and 1215 ± 20 million years old. Although nonbiological origins for the discoidal impressions cannot be completely discounted, the structures resembling trace fossils clearly have a biological origin and suggest the presence of vermiform, mucus-producing, motile organisms.

The absence of uncontroversial animal fossils older than the Ediacaran biota has led to the prevalent view among paleontologists that the first crown-group metazoan (i.e., the last common ancestor of the smallest clade to contain all extant branches of animals) was not much older than ~600 million years (*1*–*3*). Metazoan-like trace or body fossils have been reported from considerably older rocks [e.g., (*4*)]; however, these have generally been reinterpreted as being inorganically produced or as fossils that are unconnected with metazoans (*2*, *5*). Molecular sequence comparisons have yielded a wide diversity of ages for the initial divergence of crown-group metazoans, ranging from ~700 to >1500 million years old (Ma) (*6*–*8*). Whatever the reasons for these discrepancies, the Precambrian fossil record needs to be critically scrutinized to evaluate the viable but controversial possibility of a long cryptic evolution of early metazoans (*9*).

The Stirling Range Formation of southwestern Australia (Fig. 1) is one of many Precambrian sedimentary successions that lack rocks suitable for dating by established techniques. The unit consists of >1600 m of quartz sandstone and shale (*10*, *11*) that have undergone subgreenschist to lower greenschist facies metamorphism and several generations of deformation (*12*, *13*). Before the discovery of presumed Ediacaran discoidal fossils (*14*–*16*), the sedimentary rocks were thought to have been deposited before 1312 Ma and metamorphosed at 1126 ± 40 Ma, on the basis of Rb-Sr whole-rock analyses (*17*).

We collected samples from the least deformed and metamorphosed region of the Stirling Range Formation (Fig. 1). The rocks contain several horizons with disk-shaped structures (<3 cm in diameter) and a single surface with trace-like fossils. Some of our geochronological samples are from the same sedimentary horizon as the disks. The rocks bearing the disks and the trace-like fossils are fine- to coarse-grained, plane-bedded sandstones with intercalated shale. The whole unit appears to have been deposited in a tide-dominated, shallow marine environment (*14*).

The trace-like fossils (Fig. 2) are preserved in convex hyporelief on the flat sole of a thick bed of fine-grained sandstone at Barnett Peak (*18*). They consist of fine ridges, ~0.5 to 1 mm wide and high, cast in sand similar to that of the overlying bed. The ridges tend to form parallel-sided pairs that are 1.5 to 2 mm wide and up to >2 cm long. The ridge pairs may be straight, but they usually curve irregularly. Occasionally, there is a central elevation between them, running as a weaker ridge for part of the distance. There is no evidence of deeper penetration into the underlying sediment. Most of the longer ridge pairs do not preserve any terminations, but in some cases, the ridges in a pair come together in a "U"-shaped ending ("u" in Fig. 2D). In one place (the black trace indicated by the arrow in Fig. 2F), such a U-shaped bend is preserved as a concave, rather than convex, structure. The ridge pairs that appear to be the best preserved (Fig. 2, G and H) have a characteristic morphology, with the ridges at one end coming together in a U shape and the ridges at the other end flaring to a width of ~3.5 mm before terminating. The collected sample contains at least 10 specimens (marked by "G," "H," "u," and "x" in Fig. 2, B, D, and F) that are closed at one end and open at the other; more of these specimens were noted in the rock outcrop. No observed specimens are closed at both ends. The ridge pairs appear to show crosscutting (examples indicated by arrows in Fig. 2, D and F). Because of the preservation in sand, it is not possible to determine the exact nature of the crosscuts.

We considered a number of nonbiological explanations for these markings. Structures formed by the breakup of a soft sheet, such as a bacterial mat, even if occasionally rolled into tubes, would be dominated by irregular, contorted, and twisted structures. The straight course of some of the ridge pairs (Fig. 2, C and D, central part) might suggest fragmented and partly folded laminae of an earlier deposited rock, the edges of which cemented the surrounding sand grains to form the distinct double ridges. However, in no case do we see the expected rectangular terminations where the laminae have been broken; also, the irregularly winding course of several ridge pairs, the apparent crosscutting, and the distinctive shape of the best-preserved specimens weigh against such an interpretation. The possibility of current-produced toolmarks is excluded because, with few exceptions (Fig. 2, C and D, center), the ridge pairs do not show parallel alignment among themselves. Finally, nothing in the habit of the observed markings resembles other known sedimentological structures, such as swash marks, rill marks, or shrinkage cracks.

The irregular but pervasive shapes and constant dimensions of the markings are strong evidence for a biological origin. The ridges closely follow the basal surface of the sandstone bed, without evidence of deeper penetration; thus, they are likely to represent structures that existed on the sediment surface before it was covered by the sand. Be-

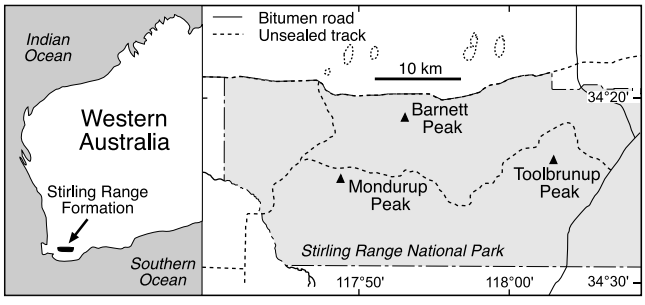

Fig. 1. Location of the Stirling Range Formation and sample sites (black triangles).

[1]Centre for Global Metallogeny, Department of Geology and Geophysics, University of Western Australia, Crawley, Western Australia 6009, Australia. [2]Department of Palaeozoology, Swedish Museum of Natural History, Box 50007, SE-104 05 Stockholm, Sweden.

*To whom correspondence should be addressed. E-mail: brasmussen@geol.uwa.edu.au

cause the ridges appear as pairs that may continue for centimeters, it is likely that ridge pairs, rather than individual ridges, represent the basic unit of the structures. These units are never closed at more than one end; thus, they are not likely to represent oblique sections through tubular walls or sections through walled bodies, such as the stacked sausage-like chambers of the Ediacaran problematic fossil *Palaeopascichnus* (*19*). A trace fossil interpretation of the Stirling structures therefore seems more likely. The course of the ridge pairs, combining both straight and irregularly curved portions, is characteristic of organisms moving on or through sediment. The crispness and well-defined dimensions of the ridges, the indication of a concave preservation in one place (Fig. 2F, arrow), and, in particular, the presence of a U-shaped termination suggest that the ridges are not negative impressions of furrows in the sediment but are positive casts of strings of a substance that eventually became filled by sand.

In order to leave such distinct casts, the ridges would have been reinforced by organic material, although no direct evidence for organic matter is seen. There is no sign of a microbial mat covering the surface, so the organic material was probably produced by the organism itself. Substrate reinforcement by mucus is a common phenomenon in animals living on or in sediment (*20*, *21*). Together with the evidence that the structures did not penetrate deep into the underlying bed, these observations suggest that the ridges are casts of mucus-impregnated strings of sediment left by an organism creeping over the surface.

Identifying the maker of a trace fossil is difficult, even in Phanerozoic rocks. Although the Stirling structures are larger than most unicellular organisms, some symbiont-carrying benthic foraminifera may reach up to several centimeters in diameter. Foraminifera may be motile and can displace sediment while moving through it (*22*). However, the small body volume of foraminifera and other unicellular protists would not allow them to produce the amounts of mucus needed to bind the long strings that we observed. If anything, protists and other small meiofauna tend to destroy rather than produce trace fossils (*20*). The required quantities of mucus indicate a vermiform organism, considerably longer than it is wide, so as to be able to sustain the necessary number of mucus glands. Furthermore, the widening of the open ends of some of the trails suggests that the body could change shape.

Mucus-producing, worm-shaped animals capable of strong distortions of body shape are well known from modern fauna; examples include nemerteans, or ribbon worms (also known as slime worms). Animals that use mucociliary motion often produce slime trails forming parallel double ridges, which may harden into three-dimensional ribbons (*21*).

We thus interpret the Stirling structures as having been produced by the surface movements of a vermiform organism with well-developed mucus-producing capacity and probably a hydrostatic skeleton. The organism began its trail by pushing forward along the sediment surface while narrowing its body from several millimeters to ~1 mm, forming a trail of parallel ridges consisting of mucus and displaced sediment. The U-shaped endings were formed where the organism was stopped in its trail (for example, by being buried in sediment) or abandoned it.

Putative body fossils in the Stirling Range Formation were described in detail by Cruse and Harris (*15*). Also at Barnett Peak, where the trace-like structures were found, up to 16 circular imprints are preserved on the upper surface of a medium- to coarse-grained, plane-bedded sandstone. The best-preserved imprints have a central tubercle surrounded by annular grooves, and they were assigned to the Ediacaran species *Cyclomedusa davidi* by Cruse and Harris [figure 2 in (*15*)]. Other discoidal structures reported by Cruse and Harris [figures 3B and 4 in (*15*)] were compared with *Cyclomedusa* and the ichnogenus *Bergaueria*.

Circular structures may have many different, including nonbiological, origins. Diagenetic marcasite nodules can produce centimeter-sized, striated structures, which have been mistaken for medusae in the past (*5*). Such nodules were probably responsible for reduction spots in shale beds elsewhere in the section, but they differ in color, size, and shape from the circular imprints interpreted as fossils. Fluid evasion marks can also produce discoidal structures, but the undisturbed laminae underlying the specimens give no evidence of fluid escape (*15*). Structures pro-

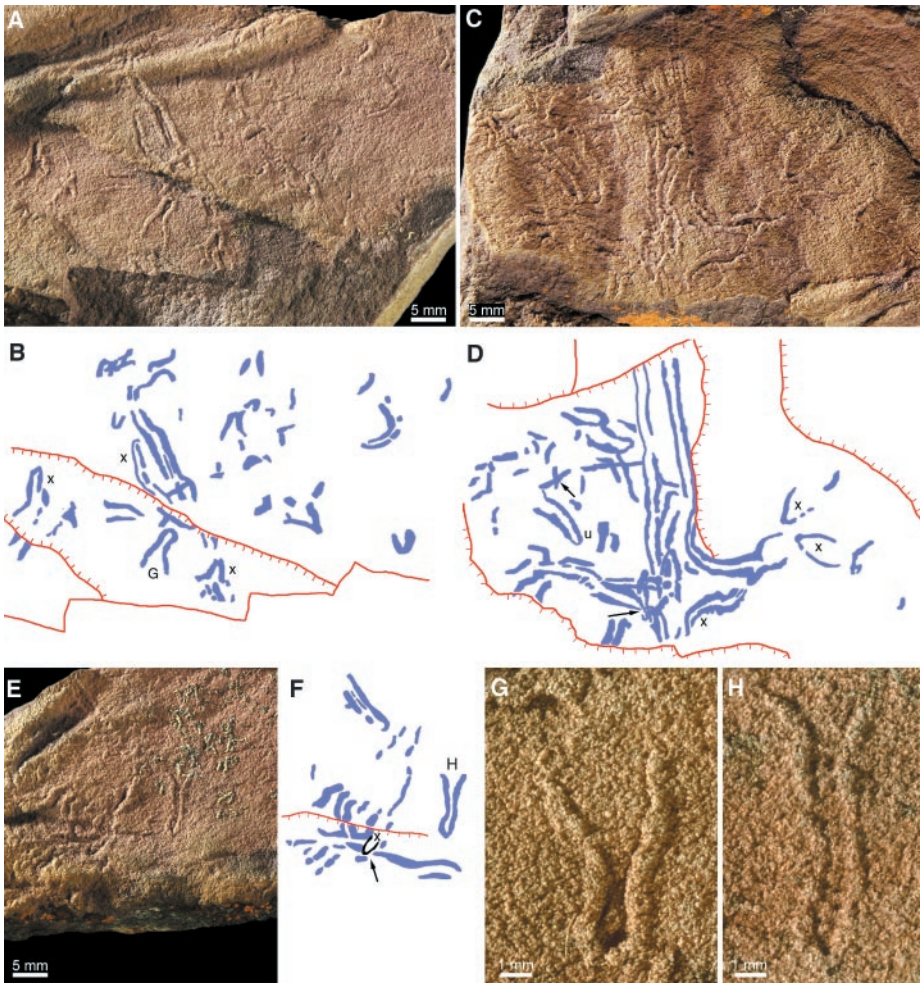

Fig. 2. Trace-like fossils, locality Barnett Peak, positive hyporelief, UWA 114336. (**A**, **C**, and **E**) Overviews of surfaces with double-ridged trails. There is low-angle lighting from the left, and the samples are shown at the same magnification. (**B**, **D**, and **F**) Drawings showing the extent of ridges (blue). Fractures and microfaults on the surface are indicated in red, specimens with a U-shaped ending are marked with the letters "u" and "x," and arrows point to instances of apparent crosscutting [black U-shaped ending "x" in (F) is in concave preservation]. (**G** and **H**) Close-ups of specimens [compare positions in (B) and (F)] with U-shaped and open expanding ends. The specimens are coated with ammonium chloride, and there is low-angle lighting from the left.

duced by bacterial (*23*) or algal (*24*) colonies may also have this general shape, but such an origin seems incompatible with the morphology and elevated relief of the imprints, as well as their preservation on a high-energy bedding plane displaying primary current lineation. Furthermore, despite repeated searches, no evidence for stromatolites or microbial mats has been found.

For these reasons, the structures are interpreted as imprints of discoidal organisms. However, given the poor state of preservation and the simple morphologies involved, taxonomic identifications with known discoidal forms are not possible. Preservational varieties of a simple, bag-shaped organism can account for most of the diversity seen among the Ediacaran discoidal fossils (*19*), and this holds true for the Stirling fossils as well.

We searched for detrital and metamorphic minerals to determine the maximum and minimum depositional ages, respectively, of the sedimentary succession. Detrital zircon grains are abundant in every sample. The only metamorphic mineral found to be suitable for U-Th-Pb geochronology was monazite, which is present as minute, euhedral crystals (<100 μm) within the sandstone matrix and as irregular, pore-filling cement. Most crystals consist of a rounded core surrounded by an inclusion-rich rim (Fig. 3A).

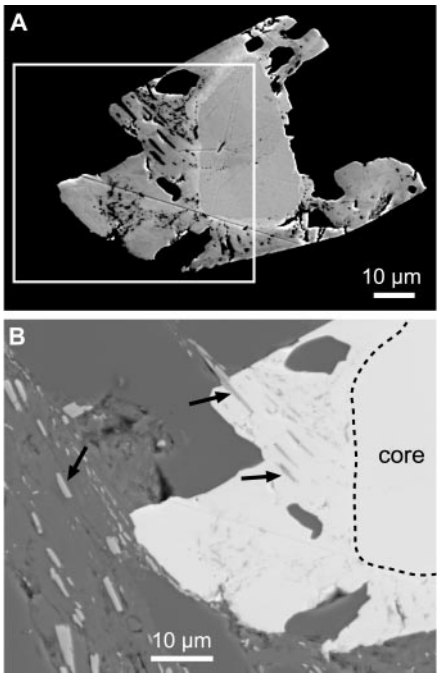

Fig. 3. (**A**) High-contrast, back-scattered scanning electron micrograph of a monazite crystal, comprising a round core and irregular, inclusion-rich overgrowth. (**B**) Close-up of the monazite overgrowth (white), containing metamorphic laths of iron oxide (gray) (indicated by arrows). The dashed line denotes the boundary between the core and the overgrowth.

Some monazite rims are partly intergrown with detrital and authigenic minerals suggestive of in situ growth. In a few samples, monazite crystals engulf minute hematite laths that are oriented with the deformational fabric (Fig. 3B), consistent with growth during or after deformation and metamorphism (*25*).

The monazite rims contain uniformly low concentrations of U [4 to 44 parts per million (ppm)], in contrast with the cores [230 to 4664 ppm; supplementary table 4 (*25*)], consistent with low-temperature growth (*26*, *27*). The high U content of the monazite cores is more suggestive of magmatic derivation and a detrital origin.

Monazite overgrowths larger than 15 μm were cut from polished thin sections, whereas zircon grains were separated from samples with conventional heavy liquid and magnetic separation techniques. Both minerals were dated with SHRIMP II (sensitive high-resolution ion microprobe mass spectrometer), according to established analytical procedures developed for monazite (*27*, *28*) and zircon (*29*).

The U-Pb data for detrital zircon grains (82 analyses on 82 grains) give ages ranging back to 3464 ± 17 Ma [supplementary table 1 (*25*)]. The youngest 23 grains yield a pooled $^{207}Pb/^{206}Pb$ age of 2016 ± 6 Ma (95% confidence level; mean square weighted deviation = 0.99), providing a maximum age for deposition.

Monazite cores (20 analyses of 13 grains) give $^{207}Pb/^{206}Pb$ ages between 1893 ± 3 and 2257 ± 18 Ma [supplementary table 4 (*25*)].

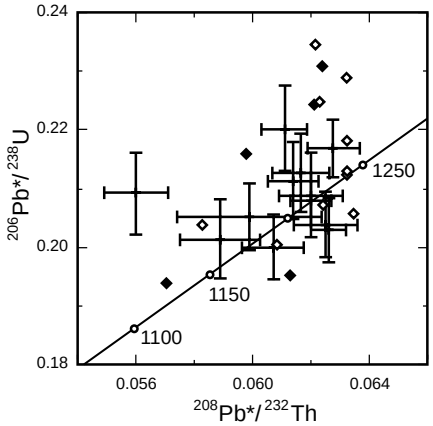

Fig. 4. U-Pb/Th-Pb concordia plot of data for metamorphic monazite overgrowths. Pb* indicates radiogenic component of measured Pb. Crosses represent data corrected for <2.5% common Pb in ^{208}Pb and <12% in ^{206}Pb, with 1σ error bars; filled diamonds represent data corrected for up to 4% common Pb in ^{208}Pb and 20% in ^{206}Pb; open diamonds represent up to 49% common Pb in ^{206}Pb and 13% in ^{208}Pb. One analysis with 43% common ^{206}Pb plots above the scale shown, and another with 18% common ^{208}Pb plots to the right of the scale shown.

Two analyses of a single monazite core yield an age of ~1895 Ma, some 100 million years younger than the youngest zircon population. Although this grain may have been derived from a younger source terrain, we used the more conservative age of 2016 ± 6 Ma as a maximum for deposition, because it is defined by a large population of zircon grains and is also supported by the bulk of the monazite core data.

U-Th-Pb analyses of monazite overgrowths (29 analyses of 14 crystals) yield indistinguishable U-Pb and Th-Pb ages (Fig. 4), which give a weighted mean of 1215 ± 20 Ma [95% confidence level; supplementary table 4 (*25*)]. The monazite overgrowths are therefore ~700 million years younger than the youngest monazite cores, consistent with postdepositional growth, as inferred from the common development of euhedral crystal faces, alignment of planar faces with cleavage direction, and intergrowth with metamorphic minerals.

The age of monazite growth in the Stirling Range Formation corresponds with the timing of monazite growth (~1200 Ma) in nearby amphibolite facies metasedimentary rocks of the Mount Barren Group (*30*) and is also synchronous with a major tectonothermal event (~1190 Ma) in the region (*31*). It is also bracketed by Rb-Sr dates (1312 and 1126 Ma) derived from slates elsewhere in the Stirling Range Formation (*17*) and is consistent with results from more recent Rb-Sr dating [~1190 Ma (*32*)]. Thus, we interpret 1215 ± 20 Ma to be the age of metamorphism, and therefore the Stirling fossils must be older.

In a Phanerozoic or Ediacaran setting, the biological and even metazoan nature of the Stirling assemblage would hardly be in doubt. Although nonmetazoan and even nonbiological interpretations are possible for the disk-shaped structures, these had been considered as Ediacaran (*15*, *16*). The trace-like fossils may be challenged as traces, but their biological origin is not in doubt. If indeed they are traces of vermiform, mucus-producing, motile organisms, three alternative conclusions may explain their early occurrence. The most conservative one is that, by 1200 million years ago, one or several multicellular or syncytial, now extinct, lineages had evolved from protist ancestors, independently of the later appearing metazoan clade. The second is that metazoan multicellularity was in existence by ≥1200 million years ago and that the trace-like fossils, and possibly the body fossils, represent one or several extinct lineages that branched off before the now living groups diversified, i.e., they are stem-group metazoans. This alternative demands that motility in metazoans evolved several times, because nonmotility is shared by the apparently paraphyletic sponges occupying the base of the metazoan crown clade (*33*). The third conclusion is that the structures

indeed represent traces of crown-group metazoans. The evidence is currently insufficient to decide between the three.

The Stirling biota offers a glimpse of a biosphere >1200 million years ago, which was more complex than the singularly microbial-algal world that is usually assumed. If our interpretation of the biota is correct, there is a challenge for paleontologists and geobiologists to find plausible mechanisms that prevented a biosphere evidently containing large motile organisms from erupting into Phanerozoic-type diversity until >600 million years later, during the Cambrian explosion. Extreme environmental conditions during the late Neoproterozoic (*34*) may have been the final bottleneck before which no diversification of organisms with metazoan-like modes of life could have had lasting success.

References and Notes

1. J. W. Valentine, D. Jablonski, D. H. Erwin, *Development* **126**, 851 (1999).
2. G. E. Budd, S. Jensen, *Biol. Rev. Camb. Philos. Soc.* **75**, 253 (2000).
3. S. Conway Morris, *Proc. Natl. Acad. Sci. U.S.A.* **97**, 4426 (2000).
4. A. Seilacher, P. K. Bose, F. Pflüger, *Science* **282**, 80 (1998).
5. P. Cloud, *Geology* **1**, 123 (1973).
6. G. A. Wray, J. S. Levinton, L. H. Shapiro, *Science* **274**, 568 (1996).
7. L. Bromham, A. Rambaut, R. Fortey, A. Cooper, D. Penny, *Proc. Natl. Acad. Sci. U.S.A.* **95**, 12386 (1998).
8. F. J. Ayala, A. Rzhetsky, F. J. Ayala, *Proc. Natl. Acad. Sci. U.S.A.* **95**, 606 (1998).
9. A. Cooper, R. A. Fortey, *Trends Ecol. Evol.* **13**, 151 (1998).
10. P. C. Muhling, A. T. Brakel, *Mount Barker–Albany, WA, 1:250,000 Geological Series Explanatory Notes* (Geological Survey of Western Australia, Perth, 1985).
11. J. S. Myers, in *Geology and Mineral Resources of Western Australia* (Geological Survey of Western Australia, Perth, 1990), pp. 255–264.
12. J. Beeson, thesis, University of Western Australia, Crawley (1991).
13. C. A. Boulter, *J. Struct. Geol.* **1**, 207 (1979).
14. T. Cruse, thesis, University of Western Australia, Crawley (1991).
15. _____, L. B. Harris, *Precambrian Res.* **67**, 1 (1994).
16. _____, L. B. Harris, B. Rasmussen, *Aust. J. Earth Sci.* **40**, 293 (1993).
17. A. Turek, N. C. N. Stephenson, *J. Geol. Soc. Aust.* **13**, 449 (1966).
18. Specimens were found by B.R. and are referred to as cf. *Palaeobullia* in (*14*), pp. 42 and 45.
19. J. G. Gehling, G. M. Narbonne, M. M. Anderson, *Palaeontology* **43**, 427 (2000).
20. R. Bromley, *Trace Fossils* (Chapman & Hall, London, ed. 2, 1996).
21. A. G. Collins, J. H. Lipps, J. W. Valentine, *Paleobiology* **26**, 47 (2000).
22. H. Kitazato, *J. Foram. Res.* **18**, 344 (1988).
23. O. Rauprich *et al.*, *J. Bacteriol.* **178**, 6525 (1996).
24. M. F. Glaessner, *Lethaia* **2**, 369 (1969).
25. Supplementary notes, including details of the geochronological procedures, SHRIMP U-Pb data for detrital zircon, and SHRIMP U-Pb data for monazite cores and overgrowths, are available on *Science* Online at www.sciencemag.org/cgi/content/full/296/5570/1112/DC1.
26. J. A. Evans, J. A. Zalasiewicz, *Earth Planet. Sci. Lett.* **144**, 421 (1996).
27. B. Rasmussen, I. R. Fletcher, N. J. McNaughton, *Geology* **29**, 963 (2001).
28. G. Foster, P. Kinny, D. Vance, C. Prince, N. Harris, *Earth Planet. Sci. Lett.* **181**, 327 (2000).
29. J. B. Smith *et al.*, *Precambrian Res.* **88**, 143 (1998).
30. G. C. Dawson, B. Krapez, I. R. Fletcher, N. J. McNaughton, B. Rasmussen, in preparation.
31. L. P. Black, L. B. Harris, C. P. Delor, *Precambrian Res.* **59**, 117 (1992).
32. L. B. Harris, *J. Geol. Soc. London* **151**, 901 (1994).
33. A. G. Collins, *Proc. Natl. Acad. Sci. U.S.A.* **95**, 15458 (1998).
34. P. F. Hoffman, A. J. Kaufman, G. P. Halverson, D. P. Schrag, *Science* **281**, 1342 (1998).

35. We thank R. Bromley, T. Cruse, D. Grazhdankin, S. Jensen, J. Lipps, S. Revets, B. Runnegar, A. Seilacher, S. Sheppard, O. Tendal, and M. Whitehouse for comments and discussion and B. David, W. Kempff, A. Kennedy, P. Kinny, B. Krapez, M. Marshall, and staff members of the University of Western Australia's Centre for Microscopy and Microanalysis for assistance. Manuscript drafts were critically reviewed by S. Jensen, B. Runnegar, and A. Seilacher. This work was supported by an Australian Research Council (ARC) fellowship and grant to B.R. Samples were collected with the permission of the Western Australian Department of Conservation and Land Management. Zircon and monazite grains were analyzed with SHRIMP II, operated by a consortium consisting of Curtin University of Technology, the Geological Survey of Western Australia, and the University of Western Australia, with ARC support.

23 January 2002; accepted 26 March 2002

Female Germ Cell Aneuploidy and Embryo Death in Mice Lacking the Meiosis-Specific Protein SCP3

Li Yuan, Jian-Guo Liu, Mary-Rose Hoja, Johannes Wilbertz, Katarina Nordqvist,* Christer Höög†

Aneuploidy (trisomy or monosomy) is the leading genetic cause of pregnancy loss in humans and results from errors in meiotic chromosome segregation. Here, we show that the absence of synaptonemal complex protein 3 (SCP3) promotes aneuploidy in murine oocytes by inducing defective meiotic chromosome segregation. The abnormal oocyte karyotype is inherited by embryos, which die in utero at an early stage of development. In addition, embryo death in *SCP3*-deficient females increases with advancing maternal age. We found that SCP3 is required for chiasmata formation and for the structural integrity of meiotic chromosomes, suggesting that altered chromosomal structure triggers nondisjunction. *SCP3* is thus linked to inherited aneuploidy in female germ cells and provides a model system for studying age-dependent degeneration in oocytes.

Aneuploidy is the leading known cause of pregnancy loss and has been recorded in ~25% of all conceptions and 0.3% of all newborns (*1*). Aneuploidy in germ cells is predominantly due to aberrant female meiotic chromosome segregation, where increasing maternal age represents a well-documented risk factor. Homologous chromosomes (homologs) in meiotic cells undergo pairing (called synapsis) and recombination during which physical links, chiasmata, are established between them. Synapsis is aided by a meiosis-specific protein complex, the synaptonemal complex (SC), which comprises two axial lateral elements (AEs) and a central element (CE) (*2*). The two AEs, which colocalize with the sister chromatids of each homolog, become connected along their entire length by fine fibers called transversal filaments (TFs) at the pachytene stage of meiotic prophase I (*3*). The AE is composed of discrete protein filaments, organized by the cohesin complex (*4*) or by two meiosis-specific proteins, synaptonemal complex protein 2 (SCP2) and SCP3 (*5*). SCP3 is required for AE formation and for male fertility (*6–8*). The function of SCP3 during the meiotic cell divisions is unclear, however, because *SCP3*$^{-/-}$ male germ cells die around the zygotene stage of meiosis (*8*).

Here, we analyze the functional role(s) of SCP3 in meiotic chromosome segregation in female germ cells. Twelve-week-old wild-type and *SCP3*-deficient females were mated with wild-type males. In contrast to *SCP3*-deficient males, *SCP3*-deficient females were fertile and generated healthy offspring (Fig. 1A). However, the *SCP3*-deficient females exhibited a sharp reduction in litter size, generating on average 5.9 offspring per female, compared with 8.9 offspring for their wild-type siblings (Fig. 1A). This reduction could be due to ovarian failures, resulting in functional oocyte loss. A comparison of ovarian morphology in *SCP3*-

Center for Genomics and Bioinformatics and Department of Cell and Molecular Biology, Karolinska Institutet, SE-171 77 Stockholm, Sweden.

*Present address: Molecular Sciences, Astra Zeneca R&D, SE-151 85 Södertälje, Sweden.

†To whom correspondence should be addressed. E-mail: christer.hoog@cmb.ki.se